

Initial growth of hexagonal and cubic boron nitride: A theoretical study

J. Olander and K. Larsson

Department of Materials Chemistry, The Ångström Laboratory, Uppsala University, Box 538, 751 21 Uppsala, Sweden
(Received 17 January 2003; revised 23 May 2003; published 21 August 2003)

Adsorption of NH_3 and BBr_3 (and their decomposed fragments) onto B and N sites of $c\text{-BN}(111)$ and $h\text{-BN}(10\bar{1}0)$, has been theoretically investigated using DFT calculations under periodic boundary conditions. The purpose was to study the adsorption processes of the precursors during gentle deposition of BN thin films in order to find prerequisites for ideal growth of $c\text{-BN}$, and to simultaneously discriminate $h\text{-BN}$ growth. The present results show that adsorption of NH_3 , NH_2 , NH , N , BBr_3 , BBr_2 , BBr , and B (with three exceptions) is exothermic to either the B or N sites of $c\text{-BN}(111)$ and $h\text{-BN}(10\bar{1}0)$, respectively. The exceptions include adsorption of NH_3 to the N site of either the cubic surface or the hexagonal edge, as well as adsorption of BBr_3 to the B-rich surface of $c\text{-BN}$. In opposite to all other combinations studied, adsorption of NH_3 and BBr_3 was found to preferably lead to an ideal growth of $c\text{-BN}$.

DOI: 10.1103/PhysRevB.68.075411

PACS number(s): 68.43.-h, 68.47.Fg, 81.15.Aa

I. INTRODUCTION

Cubic boron nitride ($c\text{-BN}$) is a suitable material for many applications in modern micro-electronic devices and machine tools because of its extreme hardness, high thermal conductivity, high thermal stability and chemical inertness.¹ Thin films of the sp^3 -bonded $c\text{-BN}$ structure have mainly been grown by chemical vapor deposition (CVD) involving ion bombardment^{2,3} or by using physical vapor deposition (PVD).⁴ These thin films are generally nanocrystalline and consist of a mixture of cubic and hexagonal BN phases.² However, thin films of $c\text{-BN}$ have recently been grown epitaxially on diamond by low pressure ion-beam assisted CVD.⁵ The layered sp^2 -bonded hexagonal structure ($h\text{-BN}$), which is a ceramics material, can be obtained by more gentle CVD methods.^{6,7}

Growth of $c\text{-BN}$ has experimentally been found to occur on (111) or (001) surfaces,^{5,8,9} while $h\text{-BN}$ grows by the edges of the hexagonal planes.¹⁰ Experimental investigations of $c\text{-BN}$ surfaces structures are sparse, probably due to the difficulties in preparing $c\text{-BN}$ single crystals. However, a number of reconstruction structures of the $c\text{-BN}(111)$ and $c\text{-BN}(001)$ surfaces [including (1×1) , (2×1) , (2×2) , and (2×4)] have been theoretically studied.^{11,12} The ideal (1×1) structure of the $c\text{-BN}(111)$ surface, has been found to be stabilized by hydrogen-termination of the surface atoms.^{13,14} More specifically, hydrogen was then found to (i) maintain the sp^3 hybridization of the surface B (N) atoms and (ii) become abstracted from the growing surface and make room for a precursor species. Furthermore, fluorine has been predicted to bind too strongly to the $c\text{-BN}(111)$ surface in order to desorb without strong energetic activation, from, e.g., energetic ion bombardment.^{3,13} Growth involving energetic bombardment of the surface is likely to create rough surfaces. Surface steps and other inhomogeneities are, to various extents, also present in more gentle ALD growth processes. The present study will, however, be focused on reactions that occur on smooth areas of BN surfaces and edges.

Ammonia is widely used as the N-supplying growth pre-

cursor for CVD of BN.² It can also supply H atoms to the process. B_2H_6 is analogously a good B supplier, but it is difficult to handle experimentally. BF_3 , BCl_3 , and BBr_3 are other boron-source precursors used for CVD of BN.^{15,16} Of these three molecules, BBr_3 is the thermodynamically least stable according to the standard enthalpy of formation which is -1136 , -404 , and -240 kJ/mol for BF_3 , BCl_3 , and BBr_3 , respectively.¹⁷ BBr_3 is, hence, expected to be the most reactive of the three molecules at low temperatures and it was chosen as the B-supplying precursor in the present study. The precursors are usually thermally activated in CVD, and temperature is, hence, an important process parameter. The precursor molecules can also be activated by a hot-filament, UV light (photolysis), the formation of a plasma, etc. Different types of activation can then be used to increase or decrease the gaseous content of specific precursor species. This can be a useful tool in designing experiments where certain growth processes are enhanced and others discriminated.

Various chemical reactions occur in a CVD reactor, depending on the precursor species present in gaseous atmosphere. It is, hence, important to account for the adsorption of many different species when studying the elementary surface reactions of CVD. One way to delimit the plausible reactions is to apply atomic layer deposition (ALD). ALD is a sophisticated type of CVD, and the general concepts are similar for the two processes.¹⁸ A major difference is, however, that the precursor gases are separately introduced into the reactor in ALD. Gas phase reactions between different precursors are then avoided. Moreover, the gaseous precursors can be differently activated in order to increase the concentration of a specific species in the reaction chamber. If suitable gas-phase precursors could be produced and identified ALD of BN could be controlled at an atomic level. One way of searching for optimal precursors is by performing theoretical modelling of surface processes that take part in the layer-by-layer growth of $c\text{-BN}$.

The purpose of the present investigation was to theoretically study initial steps of $c\text{-BN}$ and $h\text{-BN}$ vapor growth from NH_3 and BBr_3 . Adsorption of these species and their decomposed fragments onto $c\text{-BN}(111)$ surface and

h -BN($10\bar{1}0$) edge sites were then investigated. An understanding of the growth processes would make it possible to favor or discriminate the growth of either c -BN or h -BN during boron nitride vapor deposition.

II. METHODS

A. General

Adsorption of NH_3 , NH_2 , NH , N , BBr_3 , BBr_2 , BBr , and B to c -BN(111) surfaces and h -BN($10\bar{1}0$) edges, respectively, have been theoretically investigated in the present study. Both B and N sites were then included. The adsorption energies were calculated using the following equation:

$$\Delta E_{\text{ads}}(A) = E(A) + E(s/e) - E(s/e-A), \quad (1)$$

where $E(s/e-A)$ and $E(s/e)$ are the calculated total energies of the surface/edge with or without an adsorbate, respectively. $E(A)$ is the total energy of the adsorbate.

The calculations, based on the density functional theory (DFT),¹⁹ were performed using the CASTEP program from Accelrys, San Diego.²⁰ In order to give reliable geometries and bond energies, the gradient corrected GGA (GGS) functional PW91 was used in describing the exchange and correlation interactions between the electrons for the closed-shell (radical) systems.²¹ Nonlocal ultrasoft pseudopotentials, in the Kleinman-Bylander separable form, were employed.²² The electronic wave functions were expanded in plane waves up to a kinetic energy of 200 (180) eV for the supercell modeling c -BN (h -BN). K points were generated according to the Monkhorst-Pack scheme.²³ Two k points were applied for the c -BN model and one k point for the h -BN model. This representation was found to be adequate for c -BN (h -BN) since the adsorption energies differed by only 2 (3)% when using 5 (2) k points and a cutoff energy of 220 eV. The difference in adsorption energies for NH (BBr) to B and N sites of h -BN was 88 (116) kJ/mol, which is close to 1 eV. These differences changed by less than 0.09 eV when using a cutoff energy of 270 eV.

B. Surface models

1. c -BN(111)

In order to describe the electronic structure of the system accurately, it is important to use (i) a large enough basis set (Sec. II A), (ii) a sufficiently large model to represent the surface, and (iii) an optimal number of geometry optimized surface atoms. Periodically repeated supercells were presently used in modeling the c -BN(111) surfaces (see Fig. 1). The two-dimensional slabs consisted of four atomic layers, each containing 3×3 atoms. The bottom and uppermost layers were saturated with hydrogen atoms and the vacuum level between the slabs was 9 Å. During the geometry optimizations, the adsorbate-binding surface atom, as well as its closest neighbors in the x , y , and z directions, were allowed to relax. The rest of the cell was fixed in order to hold the characteristics of the underneath bulk. In order to justify the usage of this specific supercell, the adsorption energy of NH_3 to the B-rich surface of c -BN(111) was calculated using a

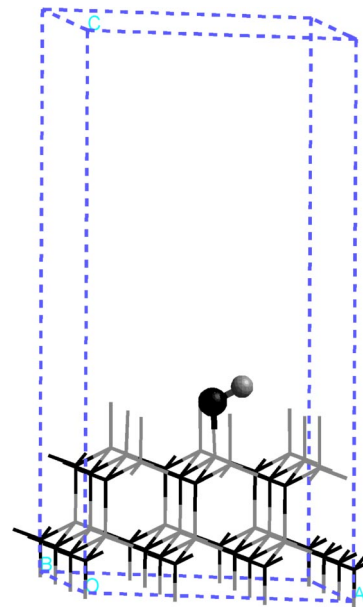


FIG. 1. A side view of the supercell modeling c -BN(111) with NH adsorbed to a B surface atom. The N atoms are black, while the B and H atoms are colored gray. The adsorbate atoms are represented by balls.

larger cell containing six atomic layers (instead of four). Each layer was then extended to contain 3×4 instead of 3×3 atoms in the x and y directions, and the two nearest neighbors were allowed to relax. Since the adsorption energies thus obtained differed by less than 5%, the smaller supercell was considered to be adequate to use in describing the c -BN(111) surface.

At the MP2 order of theory, one of the present authors has earlier calculated the adsorption energy of H to c -BN(111) to be 442 kJ/mol (compared to 437 kJ/mol presently obtained).¹³ Furthermore, the adsorption energy of NH_2 was calculated to be 459 kJ/mol (compared to the present value of 451 kJ/mol). Hence, the present results obtained by using DFT give results similar to the very accurate MP2 method. This is an additional verification of the accuracy of the computational method used in the present study.

2. h -BN($10\bar{1}0$)

Hexagonal boron nitride consists of sp^2 -bonded BN sheets that are held together by van der Waals forces. In the supercell presently modelling h -BN($10\bar{1}0$), the ideal interplanar distance of 3.3 Å was applied (Fig. 2). In this model, the hexagonal sheets were infinitely extended in one direction and H terminated in the other. Moreover, the vacuum layer between two H-terminated edges was 7 Å. During the geometry optimizations, the atoms of the BN sheet, closest to the adsorbate-binding B (N) edge atom, were allowed to relax. In order to verify this model, the adsorption energy of BBr_2 was calculated using a slab consisting of 24-atom sheets and a 9 Å thick vacuum layer. The two closest neighbors to the binding edge atom were then geometry optimized. Since the resulting adsorption energy differed by

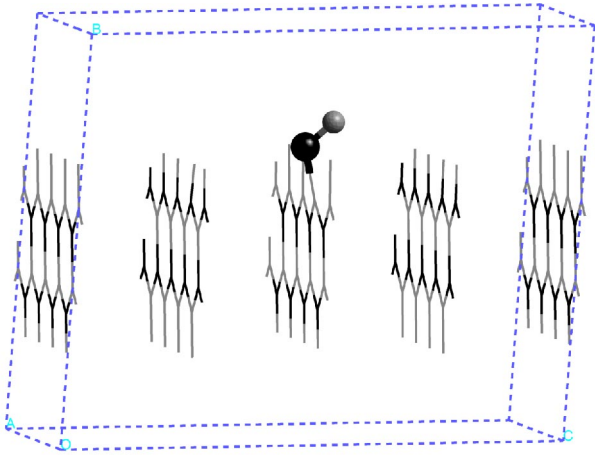


FIG. 2. A side view of the supercell modeling h -BN($10\bar{1}0$) with NH adsorbed to a B edge atom. The N atoms are black, while the B and H atoms are colored gray. The adsorbate is represented by balls.

about 1%, the primarily described model was considered to be adequate in representing the h -BN($10\bar{1}0$) edge.

III. RESULTS AND DISCUSSION

A. Introduction

Many competing surface reactions occur during ALD of various materials. These reactions are both very dynamic and complex. Gaseous molecules become adsorbed to the surface. Adsorbed molecules migrate on the surface, or become abstracted. In order to obtain a deeper knowledge of a feasible ALD experiment of c -BN, adsorption reactions of NH_3 and BBr_3 on surfaces (edges) of cubic (hexagonal) BN have been studied. According to equilibrium thermodynamic calculations, BBr_3 is not expected to dissociate appreciably ($<0.01\%$) under the conditions of low-temperature ALD.²⁴ NH_3 , on the other hand, is predicted to decompose into the more stable N_2 and H_2 molecules. This transformation will not occur instantly and a larger portion of the BBr_3 and NH_3 species introduced into the ALD reactor can be expected to approach the growing surface. However, if the molecules will undergo additional gas phase activation they will dissociate to various extents. Irradiation with an ArF excimer laser is, for example, effective in dissociating an NH_3 to NH_2 and NH .²⁵ In ALD, the precursor dissociation can be performed to different degrees for different precursor molecules. The adsorption of NH_3 and BBr_3 , as well as the adsorption of their decomposed fragments, to c -BN(111) surfaces and h -BN($10\bar{1}0$) edges has, for this reason, presently been investigated. For the sake of clarity, the various results are here presented in three different groups: (i) Hybridization of non-terminated surface (or edge) atoms, (ii) adsorption of N, NH, NH_3 , NH_2 , and (iii) adsorption of B, BBr, BBr_2 , and BBr_3 .

B. Hybridization of nonterminated surface or edge atoms

1. General

A factor that strongly influences the surface processes during growth is the surface coverage of terminating atoms.

TABLE I. The angle between the adsorbate-binding surface/edge B(N) atom and its closest N(B) neighbors; $\nu_{\text{N-B}(\text{surface/edge})\text{-N}}$ ($\nu_{\text{B-N}(\text{surface/edge})\text{-B}}$).

	c -BN(111)		h -BN($10\bar{1}0$)	
	$\nu_{\text{N-B}(\text{surface})\text{-N}}$	$\nu_{\text{B-N}(\text{surface})\text{-B}}$	$\nu_{\text{N-B}(\text{edge})\text{-N}}$	$\nu_{\text{B-N}(\text{edge})\text{-B}}$
Rad.	117.9	111.0	124.3	135.1
N	108.5	106.1	122.9	119.3
NH	106.3	106.6	121.1	122.5
NH_2	106.0	107.5	120.3	124.3
NH_3	109.6	111.3	125.6	132.7
H	107.7	108.3	122.0	124.0
B	108.7	104.4	122.9	121.2
BBr	108.0	104.3	121.2	120.0
BBr_2	104.7	100.9	120.4	118.3
BBr_3	103.6	101.9	116.0	116.2
Br	107.7	112.4		

One of the desirable roles of these terminating species during growth of c -BN is to maintain the sp^3 hybridization of the surface atoms. The surface atoms are thereby prevented from collapsing to the sp^2 hybridization of the hexagonal phase. The terminating atoms should also leave room for incoming B- or N-containing growth species in order for a continuous c -BN growth to occur. One of the present authors has earlier found H and F to be effective in stabilizing the sp^3 hybridization of the B(111) and N(111) surfaces of c -BN.^{13,14} Moreover, hydrogen atoms on a H-terminated surface were then found to become more easily abstracted by gaseous H or F radicals compared to terminating fluorine atoms on a F-terminated surface. In addition, H atoms were (compared to F atoms) found to be much more mobile on the BN surface. Hence, hydrogen is a good candidate for terminating c -BN surfaces. Hydrogen is generally also assumed to stabilize the sp^2 hybridization of hexagonal BN edges.

2. c -BN(111)

The abstraction of one terminating H atom from the hydrogenated B(111) surface of c -BN resulted in a highly distorted sp^3 hybridization of the unterminated B atom. According to the calculated $\nu_{\text{N-B}(\text{surface})\text{-N}}$ angle (117.9° ; Table I), the unterminated surface atom was almost completely sp^2 hybridized (i.e., almost 120°). One reason for this distortion of the cubic structure is that the surface B atom (which has only three valence electrons) enhances its surrounding electron density by relaxing downwards. Adsorption of either H (or Br) resulted in a retained sp^3 hybridization of the binding surface B atom ($\nu_{\text{N-B}(\text{surface})\text{-N}} = 107.7^\circ$). Moreover, the adsorption energies of either H or Br were found to be as large as 436–437 kJ/mol (Table II). Hence, in accordance with earlier studies, both H and Br were found to be efficient in stabilizing the B(111) surface of c -BN.^{13,14}

Abstraction of a surface-terminating H atom from the N(111) surface resulted in an almost maintained sp^3 hybridization of the unterminated N atom. The $\nu_{\text{B-N}(\text{surface})\text{-B}}$ angle was found to be 111.0° (compared to the ideal value of 109.4°). It is thus likely that the cubic phase will be sus-

TABLE II. Adsorption energies (kJ/mol) for various adsorbates to B and N sites of *c*-BN(111) and *h*-BN(10 $\bar{1}$ 0), respectively.

	<i>c</i> -BN(111)		<i>h</i> -BN(10 $\bar{1}$ 0)	
	B site	N site	B site	N site
N	515	622	417	397
NH	299	475	480	392
NH ₂	451	295	436	314
NH ₃	236	-30	65	-8
H	437	465	432	490
B	368	531	367	589
BBr	331	307	358	474
BBr ₂	338	479	480	496
BBr ₃	-96	241	96	147
Br	436	392		

tained even in the situation of a not perfectly terminated N(111) surface of *c*-BN. One reason for this is that nitrogen (with five valence electrons) fulfills its valence electron shell by binding to three boron atoms. By adsorption of a H atom, the sp^3 hybridization of the surface N atom was almost ideal ($\nu_{\text{B-N}(\text{surface})\text{-B}} = 108.3^\circ$). However, unlike the situation for the B(111) surface, the binding surface N atom was partly sp^2 hybridized as a result of Br adsorption ($\nu_{\text{B-N}(\text{surface})\text{-B}} = 112.4^\circ$). The long binding distance of Br (2.31 Å; Table III) also implies steric hindrances. Hence, in spite of large adsorption energies (392–436 kJ/mol; Table II) for both H and Br to *c*-BN-N(111), only H seems to be a good terminating species. This conclusion agrees with earlier findings.^{13,14}

3. *h*-BN(10 $\bar{1}$ 0)

Upon geometry optimization of *h*-BN, including an un-terminated B edge atom in the [10 $\bar{1}$ 0] direction, $\nu_{\text{N-B}(\text{edge})\text{-N}}$ increased to 124.5° (Table I). This angle indicates a somewhat distorted sp^2 hybridization of the B edge atom. Furthermore, the sp^2 hybridization of an un-terminated N edge

TABLE III. The distance r_1 between the adsorbate and the surface/edge (Å).

	<i>c</i> -BN(111)		<i>h</i> -BN(10 $\bar{1}$ 0)	
	B site	N site	B site	N site
N	1.50	1.32	1.43	1.25
NH	1.46	1.44	1.43	1.34
NH ₂	1.45	1.48	1.47	1.43
NH ₃	1.62	3.01	1.58	2.58
H	1.20	1.03		1.01
B	1.76	1.35	1.70	1.35
BBr	1.73	1.40	1.68	1.38
BBr ₂	1.86	1.41	1.74	1.44
BBr ₃	1.96	1.61	1.82	1.49
Br	2.01	2.31		

atom was largely distorted ($\nu_{\text{B-N}(\text{edge})\text{-B}} = 135.1^\circ$, which differs considerably from the ideal value of 120°). By adsorption of an H atom, the sp^2 hybridization of the binding B or N atom was, however, recovered to a certain extent ($\nu_{\text{N-B}(\text{edge})\text{-N}}/\nu_{\text{B-N}(\text{edge})\text{-B}} = 122.0^\circ/124.0^\circ$). Moreover, the large adsorption energies (432–490 kJ/mol, Table II) obtained for H, adsorbed to the B and N edge atoms of *h*-BN(10 $\bar{1}$ 0), imply that the corresponding bonds will be very strong, if not completely ideal.

C. Adsorption of N, NH, NH₂, and NH₃

1. Adsorption to *c*-BN-B(111)

Adsorption of N, NH, NH₂ and NH₃ to the B-rich surface of *c*-BN(111) was primarily studied in this paper (Table II). The numerical order of the calculated adsorption energies is

$$\text{N}(515) > \text{NH}_2(451) > \text{NH}(299) > \text{NH}_3(236). \quad (2)$$

The numbers within parenthesis show the calculated exothermic adsorption energies in kJ/mol. Accordingly, the adsorption energies were found to be strongly exothermic. The results indicate (with one exception) that the more dissociated the precursor is, the stronger it adsorbs, although the order of NH and NH₂ was reversed relative to this general trend. Moreover, a strong correlation was found between the obtained energies and the r_1 distance (the distance between the binding surface B atom and the N atom in the adsorbate). As the adsorption energies decreased with an increasing number (0–3) of H atoms in the adsorbate, r_1 increased (from 1.32 to 1.62 Å; Table III).

For an ideal layer-by-layer growth of *c*-BN, it is critical to preserve the sp^3 hybridization of the adsorbate-binding atom. As a result of the present adsorption processes, the sp^3 hybridization of the binding surface B atoms was maintained. More specifically, the angles $\nu_{\text{N-B}(\text{surface})\text{-N}}$ in the geometry optimized models were calculated to be between 103.6° and 109.6° (Table I).

Experimental temperatures, that are used during deposition of thin films, will influence adsorption reactions. However, if the difference between two adsorption energies is larger than ~1 eV, the order of these energies is not expected to alter with an increase in temperature. Hence, the large adsorption energies (and favorable adsorption geometries) presented here indicate that NH₃ and its decomposed fragments are promising precursor candidates for growth of *c*-BN(111) even at experimental deposition temperatures.

2. Adsorption to *c*-BN-N(111)

Adsorption to the N(111) surface of *c*-BN was also studied in the present investigation, and the following order of adsorption energies was obtained:

$$\text{N}(622) > \text{NH}(475) > \text{NH}_2(295) \gg \text{NH}_3(-30). \quad (3)$$

All adsorption reactions were, with one exception, found to be strongly exothermic. The exception includes adsorption of gaseous NH₃ to the N(111) surface, which was found to be endothermic (-30 kJ/mol) and thus unlikely to occur. The

N atom in ammonia is initially surrounded by eight valence electrons and it is, hence, not further stabilized by the addition of two extra valence electrons [which it would receive as a result of binding to the N(111) surface]. Generally, the adsorption energies were found to be considerably stronger for the more dissociated adsorbates. Moreover, the differences between the calculated energies were larger compared to the B(111) surface (Sec. III C 1). Adsorption of N or NH was even found to be more favorable for this N-rich surface than for the B-rich surface. Decreasing adsorption energies could clearly be correlated to lengthened bond distances (r_1), ranging from 1.32 Å (for N) to 3.01 Å (for NH₃; Table III).

For each of the exothermic adsorption reactions, the sp^3 hybridization of the binding surface N atom was preserved. The angle $\nu_{\text{B-N(surface)-B}}$ was, after adsorption of N, NH, or NH₂, found to be 101.9–107.5° (Table I). For the nonbinding NH₃ species, the corresponding angle (111.3°) was similar to the one obtained for the unterminated surface N atom (111.0°). This is in accordance with the endothermic adsorption reaction of NH₃, which implies that it will not bind.

In summary, N and NH were found to adsorb stronger to the N-rich surface of *c*-BN(111) while NH₂ and NH₃ were found to adsorb stronger to the B-rich surface. Adsorption of N and NH would, hence, preferably result in N-N bonds in the growing film. Such bonds are not present in an ideal BN structure, where all N atoms bind to four (or three) B atoms. NH₂ and NH₃ are, hence, more favorable than N and NH for ideal layer-by-layer growth of BN films.

3. Adsorption to a B edge atom of *h*-BN(10 $\bar{1}$ 0)

Adsorption to a hexagonal BN edge atom in the (10 $\bar{1}$ 0) direction has also been investigated. In this orientation of *h*-BN, the positions of the B and N atoms are inverted in successive BN sheets (Fig. 2). However, every individual hexagonal sheet ends by either B or N atoms. The order of the adsorption energies obtained for a B site is



The trend of adsorption energies differs somewhat from the ones obtained for *c*-BN(111) (Secs. III C 1 and III C 2). The most striking difference is that the radical N species does not correspond to the largest adsorption energy. Compared to the cubic B site, the adsorption energy of NH₃ was much smaller (by 171 kJ/mol). For the B edge, the differences in adsorption energies between the N, NH, and NH₂ species were not large (<63 kJ/mol) and the r_1 bond lengths of the N and NH species were found to be identical (1.43 Å; Table III). For the remaining adsorbates, r_1 increased with the number of H atoms in the adsorbate. The observation that the N species did not form a shorter bond (than NH) to the surface agrees with the fact that it did not correspond to the largest adsorption energy (of the four adsorbates studied).

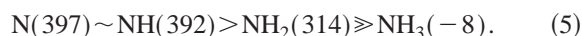
The $\nu_{\text{N-B(edge)-N}}$ angle for the adsorbate-binding B atom was 120.3°–122.9° after adsorption of N, NH, and NH₂, respectively (Table I). Upon adsorption of NH₃, $\nu_{\text{N-B(edge)-N}}$ (124.5°) was similar to that of an unterminated B atom

(125.6°). This is in accordance with the small adsorption energy and long bond distance obtained for NH₃, implying that it will not adsorb.

In summary, N was found to bind weaker to *h*-BN-B(10 $\bar{1}$ 0) compared to the cubic surfaces studied, whereas NH and NH₂ formed bonds of similar (or higher) strength to the hexagonal B site. The adsorption of NH₃ to *h*-BN-B(10 $\bar{1}$ 0) or *c*-BN-N(111) was only slightly exothermic (or endothermic), compared to the distinctly exothermic reaction for *c*-BN-B(111).

4. Adsorption to an N edge atom of *h*-BN(10 $\bar{1}$ 0)

The order of adsorption energies obtained for the *h*-BN-N(10 $\bar{1}$ 0) edge was identical to the corresponding one for the *c*-BN-N(111) surface:



The adsorption energies obtained decreased with an increasing number of H atoms in the adsorbate. However, the adsorption energies of N and NH were very similar. The r_1 bond length increased (from 1.25 to 2.58 Å) as the adsorption energy decreased (Table III). More specifically, the r_1 distance obtained for the N adsorbate was found to be only 1.25 Å and the corresponding value for the *c*-BN-N(111) surface was 1.32 Å (Sec. III C 2). The tabulated average length of a N=N double and a N-N single bond is 1.25 and 1.46 Å, respectively.¹⁷ These values suggest that N adsorption to the cubic and hexagonal N sites resulted in double bonds rather than single bonds. Moreover, the energies for N adsorption to the *h*-BN-N(10 $\bar{1}$ 0) edge and the *c*-BN-N(111) surface were found to be as large as 397 and 622 kJ/mol, respectively. Hence, the average bond enthalpy for a N=N double bond (470 kJ/mol) corresponds better to the adsorption energies obtained for the N radical species than the enthalpy of a N-N single bond (158 kJ/mol) does.¹⁷

The $\nu_{\text{B-N(edge)-B}}$ angle of the adsorbate binding N atom increased with the number of H atoms in the adsorbate (from 119.3° for N to 124.3° for NH₂; Table I). As a result of the endothermic adsorption reaction of NH₃, $\nu_{\text{B-N(edge)-B}}$ was found to be as large as 132.7°. This is close to the angle obtained for an unterminated N atom (135.1°) and corresponds well with the observation that no NH₃ adsorption will not take place.

In summary, adsorption of the gaseous N species was found to be similar to (or stronger than) the N sites compared to the B sites of either *c*-BN(111) or *h*-BN(10 $\bar{1}$ 0). In order for an ideal BN growth to occur, the N-contributing precursors should have preferences for binding to B sites. The N radical species does, hence, not seem to be a good precursor. NH was found to bind strongly to *h*-BN-B(10 $\bar{1}$ 0) and to either of the cubic surface sites, but weaker to *h*-BN-N(10 $\bar{1}$ 0). Moreover, NH₂ was found to bind stronger (by 122–156 kJ/mol) to the B sites compared to the N sites of *c*-BN and *h*-BN, respectively. Hence, NH₂ is promising for a continued growth of either cubic or hexagonal BN, but it does not seem to discriminate growth of either of the two

phases. NH_3 was found to bind relatively strongly to the B(111) surface of *c*-BN but weakly or not at all to the remaining sites investigated. Hence, among the N-containing species included in this study, only NH_3 is a promising precursor for growth of *c*-BN rather than *h*-BN.

D. Adsorption of B, BBr, BBr_2 , and BBr_3

1. Adsorption to *c*-BN-B(111)

Adsorption of BBr_3 as well as its fragmented components was studied in the present investigation. The order of energies obtained to the B(111) surface of *c*-BN was

$$\text{B}(368) > \text{BBr}_2(338) \sim \text{BBr}(331) \gg \text{BBr}_3(-96). \quad (6)$$

The adsorption reactions of B, BBr, and BBr_2 were exothermic and the corresponding energies were found to be numerically very similar. The adsorption of BBr_3 was found to be endothermic. Moreover, the binding distance (r_1) of BBr was as short as 1.73 Å, while the bond lengths of B and BBr_2 to the surface were calculated to be 1.76 and 1.86 Å, respectively (Table III). As expected, the BBr_3 nonbinding distance was longer ($r_1 = 1.96$ Å).

Steric hindrances are generally expected to lead to lengthened bonds as well as to decreased adsorption energies. The binding surface atom can also become uplifted with a decreased angle $\nu_{\text{N-B}(\text{surface})-\text{N}}$ as a result. For all of the adsorbates presently studied, the sp^3 hybridization of the binding surface B atoms was fairly well maintained. Moreover, as a result of steric hindrances, the $\nu_{\text{N-B}(\text{surface})-\text{N}}$ angle decreased with an increasing number of Br atoms in the BBr_X adsorbate (from 108.7° for $X=0$ to 103.6° for $X=3$; Table III). Adsorption of B, BBr, and BBr_2 to the *c*-BN-B(111) surface was found to be favorable while BBr_3 adsorption can be excluded.

2. Adsorption to *c*-BN-N(111)

The adsorption processes of BBr_3 , BBr_2 , BBr, and B to the N-rich surface of *c*-BN(111) were all found to be energetically favorable. The numerical order of the obtained adsorption energies was

$$\text{B}(531) > \text{BBr}_2(484) > \text{BBr}(307) > \text{BBr}_3(241). \quad (7)$$

The adsorption reactions of B, BBr_2 , and BBr_3 on this surface were, compared to the B-rich surface, more favorable (by 110–337 kJ/mol). However, BBr was found to form equally strong bonds to either of the two surfaces. Larger adsorption energies could be correlated to shorter bond distances [$\Delta E_{\text{ads}}(\text{BBr}_3) = 241$ kJ/mol, $r_1(\text{BBr}_3) = 1.61$ Å; $\Delta E_{\text{ads}}(\text{B}) = 531$ kJ/mol, $r_1(\text{B}) = 1.35$ Å, Tables II, III].

The $\nu_{\text{B-N}(\text{surface})-\text{B}}$ angle of the binding surface N atom decreased with an increasing number of Br atoms in the adsorbate (from 104.4° for B to 100.2° for BBr_2 ; Tables I). This is probably due to increased steric hindrances for larger adsorbates, similar to the situation found for the B-rich surface (Sec. III D 1). However, $\nu_{\text{B-N}(\text{surface})-\text{B}}$ increased somewhat (to 101.9°) with a considerably longer binding distance for BBr_3 . In order to illustrate the steric situation of the

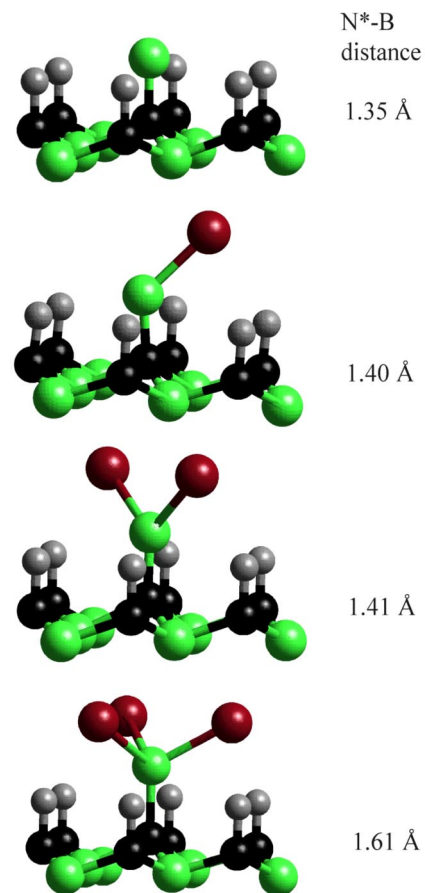


FIG. 3. The binding situation of BBr_X ($X=0-3$) on the *c*-BN-N(111) surface is illustrated by the optimized geometrical structures. The corresponding bond length between the surface N-atom (with an asterisk) and the B atom of the adsorbate, is written next to each of the figures.

B-containing adsorbates on the N-rich surface, the optimized geometries are shown in Fig. 3. Compared to $\nu_{\text{N-B}(\text{surface})-\text{N}}$ of the B(111) plane, the $\nu_{\text{B-N}(\text{surface})-\text{B}}$ angles of N(111) were smaller (by $3.7^\circ-4.3^\circ$). Generally, $\text{B}_{\text{surf}}-\text{B}_{\text{ads}}$ bonds are longer than $\text{N}_{\text{surf}}-\text{B}_{\text{ads}}$ bonds, since the covalent radii of B and N are 0.88 and 0.73 Å, respectively.¹⁷ The bromine atoms of the BBr_X adsorbate will, hence, be closer to the N-rich surface (compared to the B-rich surface) with somewhat less pronounced steric hindrances as a result.

In summary, B, BBr_2 , and BBr_3 were found to adsorb more strongly to N(111) compared to B(111). The adsorption energies of BBr to the two surfaces were quite similar. Of the four B-containing species, BBr_3 corresponded to the smallest adsorption energies. However, it was found to bind much stronger (by 337 kJ/mol) to N(111) compared to B(111), something which is promising for an ideal growth of *c*-BN. Since BBr_3 is assumed to be abundant in a deposition reactor and it may, hence, be very important for *c*-BN growth.

3. Adsorption to a B edge atom of *h*-BN(10 $\bar{1}0$)

For chemisorption of the B-containing precursors to B sites of the hexagonal (10 $\bar{1}0$) edge, the following order of adsorption energies was obtained:

$$\text{BBr}_2(480) > \text{B}(367) \sim \text{BBr}(358) \gg \text{BBr}_3(96). \quad (8)$$

As can be seen, all of the adsorption reactions were exothermic. Moreover, the order of the energies obtained for B and BBr_2 was inverted compared to the cubic surfaces. The adsorption energies for B and BBr were numerically close to the ones obtained for the B-rich plane of $c\text{-BN}(111)$ (Sec. III D 1). On the contrary, BBr_2 was found to adsorb stronger to this hexagonal B site than to either of the cubic surfaces. In spite of much larger sterical hindrances, the BBr_2 bond was only slightly longer (1.74 Å) than the corresponding one for the B species (1.70 Å; Table III).

The sp^2 hybridization of the adsorbate-binding B edge atom was maintained after adsorption of each of the B-containing precursors. Specifically, $\nu_{\text{N-B}(\text{edge})\text{-N}}$ decreased with an increasing number of Br atoms in the BBr_X adsorbate, from 122.9° (for $X=0$) to 116.0° (for $X=3$; Table I). This resembles the behavior observed for the cubic $\text{BN}(111)$ surfaces (Secs III D 1 and III D 2).

In summary, the radical B precursor was found to form energetically similar bonds to either of the B sites studied, but it bound much stronger to the cubic N site. The adsorption energies of BBr were numerically very similar for all of these three sites. Moreover, BBr_2 was found to bind stronger to $c\text{-BN-N}(111)$ and $h\text{-BN-B}(10\bar{1}0)$ compared to $c\text{-BN-B}(111)$. The adsorption reaction of BBr_3 was more strongly exothermic for the cubic N-rich site than for either of the B-rich sites studied. Hence, according to the results presented so far either B or BBr_3 would be favorable for an ideal growth of $c\text{-BN}$.

4. Adsorption to an N edge atom of $h\text{-BN}(10\bar{1}0)$

Finally, adsorption of the gaseous B-containing species to an N site of the $h\text{-BN}(10\bar{1}0)$ edge was studied. The order of the adsorption energies was identical to the ones obtained for the $c\text{-BN}(111)$ surfaces

$$\text{B}(589) > \text{BBr}_2(496) > \text{BBr}(442) \gg \text{BBr}_3(147). \quad (9)$$

The adsorption reactions of B and BBr were more favorable for this hexagonal N edge compared to the B edge. Furthermore, adsorption of either B and BBr was stronger (by 58 and 135 kJ/mol) to the hexagonal N site compared to the corresponding site on the $c\text{-BN}$ surface. BBr_2 formed bonds of similar strength to either of the hexagonal sites and to the N-rich cubic site, but it bound somewhat weaker to the B-rich cubic site. The adsorption energy of BBr_3 was smaller by 39% for the hexagonal compared to the cubic N site (Table II).

For the hexagonal N site, the BBr_X binding distance increased from 1.35 to 1.49 Å for X going from 0 to 3 (Table III). The range of bond lengths was, hence, smaller than the corresponding one obtained for the $c\text{-BN-N}(111)$ surface (Sec. III D 2). This can partially be explained by the smaller sterical hindrances present for BBr_X adsorbed to $h\text{-BN}$ compared to $c\text{-BN}$ (Figs. 1 and 2). Moreover, the angle $\nu_{\text{B-N}(\text{edge})\text{-B}}$ of the binding N edge atom decreased, as a result of BBr_X adsorption, from 121.2° to 116.2° as X increased from 0 to 3 (Table I).

In summary, the gaseous B species was found to bind much stronger to the N sites than to the B sites studied. The adsorption of BBr was energetically similar for all the investigated sites, except for the more favorable adsorption reaction to $h\text{-BN-N}(10\bar{1}0)$. Moreover, BBr_2 bound strongly to $c\text{-BN-N}(111)$, as well as to either of the hexagonal sites, but somewhat weaker to $c\text{-BN-B}(111)$. The adsorption of BBr_3 was found to be weak to the B sites. However, BBr_3 was predicted to adsorb to either of the N-rich sites investigated and to form a relatively stronger bond to the cubic surface.

IV. CONCLUSIONS

The growth of BN thin films has been theoretically investigated, using DFT calculations under periodic boundary conditions. This has been done by studying the adsorption of NH_3 and BBr_3 , and their decomposed fragments, onto $c\text{-BN}(111)$ surfaces and $h\text{-BN}(10\bar{1}0)$ edges.

As a result, almost all of the adsorption reactions were found to be exothermic. The endothermic reactions include adsorption of NH_3 to the N sites of either $c\text{-BN}$ or $h\text{-BN}$, as well as BBr_3 adsorption to $c\text{-BN-B}(111)$. For the cubic surface, NH_3 and BBr_3 corresponded to the smallest adsorption energies of the investigated precursor species. Nevertheless, they were predicted to constitute the most promising combination for gentle growth of $c\text{-BN}(111)$ surfaces by vapor deposition involving mixed precursor gases (under the assumption that the gaseous reactions between the precursors are negligible). Gaseous N, NH, and BBr species were on the other hand found to be unfavorable under such conditions. The reason was the risk of N-N and B-B bond formation. Furthermore, chemisorption of NH_2 , B, or BBr_2 were predicted to preferably form B-N bonds to $c\text{-BN}(111)$, but to also with a certain probability result in N-N or B-B bonds.

For the hexagonal edge, the adsorption of NH, NH_2 , B, and BBr was predicted to preferably lead to a continued $h\text{-BN}$ growth (involving B-N bonds). However, these species were also found capable of forming strong B-B or N-N bonds and the present results cannot reveal which adsorption reaction will be favored at elevated temperatures. The N, BBr_2 , and BBr_3 species were found to bind to both sites of the $h\text{-BN}(10\bar{1}0)$ edges with almost similar adsorption energies.

The present results suggest that there is a large probability to obtain a mixture of B-N, N-N, and B-B bonds, as a result of NH_X and BBr_X precursor adsorption to $c\text{-BN}$ and $h\text{-BN}$ ($X=0-3$). Separate precursor introduction, could prevent such a situation. Because of larger adsorption energies of the dissociated species, dissociation of the precursors was also found to favor for an ideal ALD process. However, only the undissociated NH_3 and BBr_3 molecules were predicted to exclusively lead to an ideal $c\text{-BN}$ CVD growth involving mixed precursors.

The mechanisms for BN growth are very complex. One of the most important elementary steps is the adsorption of a precursor species on the growing surface. Strongly exothermic adsorption reactions are more likely to occur than slightly exothermic ones. Moreover, endothermic adsorption

reactions will with certainty not occur. The focus of the present study was to investigate adsorption on ideal BN surfaces and edges as elementary steps in growth of the material. Another important factor to study is the presence of adsorption barriers since a large barrier of adsorption may inhibit an exothermic adsorption reaction. The migration and dissociation of an adsorbed species on the growing surface are other essential steps involved in vapor growth mechanisms. These steps are, as a continuation of the presently

studied adsorption processes, under investigation by the present authors.

ACKNOWLEDGMENT

This paper was supported by the Swedish Foundation for Strategic Research SSF Materials Research Program on Low-Temperature Thin Film Growth. The results were generated using the program Cerius2. This program was developed by Accelrys Inc., San Diego.

-
- ¹H. Erhardt, *Surf. Coat. Technol.* **74/75**, 29 (1995).
²I. Konyashin, J. Bill, and F. Aldinger, *J. Chem. Vap. Deposition* **3**, 239 (1997).
³W. Zhang, X. Jiang, and S. Matsumoto, *Appl. Phys. Lett.* **79**, 4530 (2001).
⁴T. Yoshida, *Diamond Relat. Mater.* **5**, 501 (1992).
⁵X.W. Zhang, H.-G. Boyen, N. Deyneka, P. Ziemann, F. Banhart, and M. Schreck, *Nature (London)* **1**, 1 (2003).
⁶T. Matsuda, N. Uno, H. Nakae, and T. Hirai, *J. Mater. Sci.* **21**, 649 (1986).
⁷R.T. Paine and C.K. Narula, *Chem. Rev. (Washington, D.C.)* **90**, 73 (1990).
⁸H. Sachev, *Diamond Relat. Mater.* **10**, 1390 (2001).
⁹W.J. Zhang, X. Jiang, and S. Matsumoto, *Appl. Phys. Lett.* **79**, 27 (2001).
¹⁰Q. Li, R. Zhang, L. Marks, W. Zhang, and I. Bello, *Diamond Relat. Mater.* **11**, 1416 (2002).
¹¹K. Kádas, G. Kern, and J. Hafner, *Phys. Rev.* **136**, B864 (2000).
¹²K. Osuch and W. Verwoerd, *Surf. Sci.* **345**, 75 (1996).
¹³K. Larsson and J.-O. Carlsson, *J. Phys. Chem. B* **103**, 6533 (1999).
¹⁴B. Mårild, K. Larsson, and J.-O. Carlsson, *Phys. Rev. B* **60**, 16065 (1999).
¹⁵W. Kohn and L.J. Sham, *Phys. Rev.* **140**, A1133 (1965).
¹⁶B.-J. Choi, *Mater. Res. Bull.* **34**, 2215 (1999).
¹⁷G. Aylward and T. Finlay, *SI Chemical Data* (Wiley, Singapore, 1994), 3rd ed.
¹⁸T. Suntola and J. Antson, **058**, 430 (1977).
¹⁹P. Hohenberg and W. Kohn, *Phys. Rev.* **136**, B864 (1964).
²⁰M.C. Payne, M.P. Teter, D.C. Allan, T.A. Arias, and J.D. Joannopoulos, *Rev. Mod. Phys.* **64**, 1045 (1992).
²¹J. Perdew and Y. Wang, *Phys. Rev. B* **45**, 13 244 (1992).
²²L. Kleinman and D. Bylander, *Phys. Rev. Lett.* **48**, 1425 (1982).
²³H. Monkhorst and J.D. Pack, *Phys. Rev. B* **13**, 5188 (1976).
²⁴B. Nöläng, EKVICALC, Ben Systems, 2002.
²⁵V.M. Donnelly, A.P. Baronavski, and J.R. McDonald, *Chem. Phys.* **43**, 1979 (1979).